Minimum-length chain embedding for the phase unwrapping problem on D-Wave's Pegasus Graph

Mohammad Kashfi Haghighi
Department of Electrical and Computer Engineering
University of Victoria
mohammadkashfi@uvic.ca

Nikitas Dimopoulos
Department of Electrical and Computer Engineering
University of Victoria
nikitas@ece.uvic.ca

2023 IEEE International Conference on Quantum Computing and Engineering (QCE) | 979-8-3503-4323-6/23/$31.00 ©2023 IEEE | DOI: 10.1109/QCE57702.2023.10261

***Abstract*—In this paper, we study the potential capability of quantum annealing in solving the phase unwrapping problem, an instance of hard computational problems. To solve the phase unwrapping problem using quantum annealing, we deploy the D-Wave Advantage machine which is currently the largest available quantum annealer. The structure of this machine, however, is not compatible with our problem graph structure. Consequently, the problem graph needs to be mapped into the target (Pegasus) graph, and this minor embedding significantly affects the quality of the results. Based on our experiment and also D-Wave's reports, the lower chain lengths can result in a better performance of quantum annealing. In this paper, we propose a new minor embedding algorithm that has the lowest possible chain length for minor embedding the graph of the phase unwrapping problem onto the Pegasus graph. The obtained results using this embedding strongly outperform the results of Auto-embedding provided by the D-Wave's minorminer tool both in the quality of the solution obtained and in the length of the chain.**

I. Introduction

Two-dimensional phase unwrapping is the process of recovering unambiguous phase values from a two-dimensional array of phase values known only modulo 2π rad. This problem arises when the phase is used as a proxy indicator of a physical quantity, which is the time delay between two signals in the case of interferometric SAR (InSAR) [1] and can be used to extract accurate three-dimensional topography. Phase unwrapping can be expressed as a minimum-cost flow problem [2] and solved using the TRWS algorithm [3]. Alternatively, we have formulated the phase unwrapping problem as a QUBO problem and used quantum annealing to solve it [4].

The cost (Hamiltonian) of this formulation is as per equation 1 where k_i are the labels that will determine the original phase, A is the set of pixels in the SAR image, and W_{st} are weights defining the neighbourhood structure and a_{st} is based on the wrapped phases [4].

$$E = \sum_{(s,t)\in A} W_{st}\left(k_t - k_s - a_{st}\right)^2 + \sum_{s\in A} \omega_s\left(k_s - a_s\right)^2 \quad (1)$$

Mapping the problem on the annealing machine plays a crucial role [4], [5].

In this work, we study a variety of embeddings for the phase unwrapping problem on D-Wave's Advantage architecture and experimentally study the impact of the chain length on the performance.

II. Methodology

The Pegasus graph is the underlying architecture of D-Wave's Advantage machine. The Pegasus graph includes the Chimera graph as its sub-graph. Each Pegasus unit cell consists of three Chimera unit cells. We process 2D images. Each pixel depicts the phase including the unknown label. Labels are assumed to be integers less than 4 and are represented as two-bit variables enumerated using three coordinates; the first two denoting the position in the 2D image and the third identifying the bit variable.

Figure 1(a) shows the graph of our problem for a 4×4 image.

To map the problem graph onto the Pegasus graph, we start with a sub-image of size 2×2 and then continue mapping its adjacent sub-images. Consider an image with sub-images like Figure 1(b). We start by mapping the red sub-image onto eight qubits of two Chimera unit cells in Figure 2(a).

We continue by mapping the right sub-image of the mapped one which is the yellow sub-image in Figure 1(b). We map this sub-image similarly to the red one. However, the left pixels of this sub-image are connected to the right pixels of the red one (i.e., pixel $(i, j+2)$ is connected to pixel $(i, j+1)$, and pixel $(i+1, j+2)$ is connected to pixel $(i+1, j+1)$). Consequently, we map the yellow sub-image in the lower left side of the red one as in Figure 2(b). We can map every other two horizontally adjacent sub-images with the same approach.

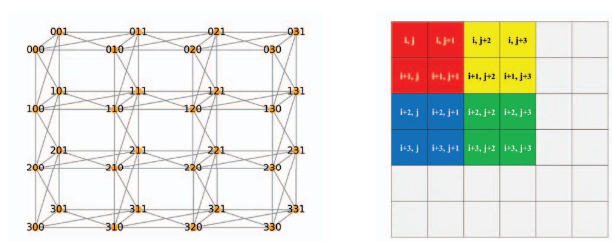

(a) Graph of the phase unwrapping problem. Nodes depict label bit-variables. The two most significant digits represent position while the least significant one represents the bit

(b) Pixels of a 4×4 images with the sub-images of size 2×2 shown in different colors

Fig. 1. Pixel locations and connections of a 4*4 image

DOI 10.1109/QCE57702.2023.10261

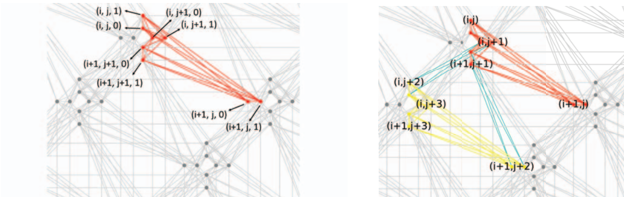

(a) 2×2 sub-image

(b) Two horizontally adjacent sub-images.

Fig. 2. Connections between bit variables are shown in red or yellow (corresponding to the separate 2x2 sub-images). turquoise edges show the connections between adjacent label variables of those sub-images.

We continue by mapping the bottom sub-images of those that were mapped (the blue and the green sub-images in Figure1(b)). These two sub-images are also horizontally adjacent and we can map them the same way as the previous adjacent sub-images. However, the top pixels of these two sub-images have connections with the bottom pixels of the previous sub-images (i.e., pixel $(i+2, j)$ is connected to pixel $(i+1, j)$, pixel $(i+2, j+1)$ is connected to pixel $(i+1, j+1)$, and so on). We map these two sub-images with a relative location with the previous ones such that these connections are provided. This is accomplished by mapping them in the lower right side of the previously mapped sub-images as Figure 3.

A Chimera cell that was partially used in the mapping of previous sub-images now is completely used as the mapping of new sub-images matched the previous one. Four sub-images are mapped so far and we can continue the same procedure to map another four sub-images. The location of the next four sub-images follows the approach that we used to map adjacent sub-images. Continuing this trend, we can map the whole image.

III. Experiments

We present experimental performance results of different minor embeddings, i.e., Native embedding (proposed in this work), and five automatically generated minor embeddings using D-Wave's Ocean minorminer tool. Table I shows their properties.

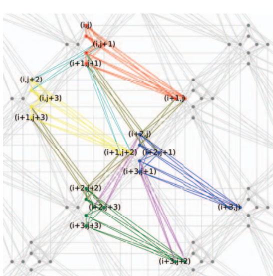

Fig. 3. Mapping four adjacent sub-image into the Pegaus graph. Connections between the blue and the green sub-images are shown in magenta. Connections between the yellow and the green and also between the red and the blue sub-images are shown in olive

We used the default annealing parameters in our experiments, i.e., annealing_time= $20\mu s$, number_of_reads $= 1000$.

Our datasets consist of 5 synthetic images with the size of 10×10 pixels with a medium noise level (SNR=10dB) and medium complexity (Perlin correlation=18) [6].

To determine how close two images (of identical size) are to each other, we use the *matching fraction* metric defined as the fraction of pixels that are identical in the two images and compare the obtained image to Noisy Unwrapped Ground-truth images [4].

In terms of chain length, our proposed Native embedding, having chain length of 1, is the optimum embedding with the lowest possible chain length. D-Wave's Ocean software couldn't find any other embedding with an average chain length of close to one (Table 1). Our proposed Native embedding results in accuracy exceeding 98% outperforming the automatically generated ones. Of the automatically generated embeddings, the one with the shorter average chain length phasor the better accuracy.

IV. Conclusion

In this work, we proposed a heuristic mapping to embed the phase unwrapping problem into the D-Wave's Advantage architecture. This embedding is optimal in terms of chain length. We experimentally showed that our embedding outperforms others confirming that a lower average-chain-length embedding would result in better accuracy.

Acknowledgment

This research was supported in part by NSERC through its Discovery, and CREATE in Quantum Computing program.

References

[1] J. C. Curlander and R. N. McDonough, "Synthetic aperture radar- systems and signal processing(book)," *New York: John Wiley & Sons, Inc*, 1991.
[2] M. Costantini, "A novel phase unwrapping method based on network programming," *IEEE Transactions on Geoscience and Remote Sensing*, vol. 36, no. 3, pp. 813–821, 1998.
[3] V. Kolmogorov, "Convergent tree-reweighted message passing for energy minimization," *IEEE Transactions on Pattern Analysis and Machine Intelligence*, vol. 28, no. 10, pp. 1568–1583, 2006.
[4] K. A. H. Kelany, N. Dimopoulos, C. P. J. Adolphs, and A. Baniasadi, "Quantum annealing methods and experimental evaluation to the phase-unwrapping problem in synthetic aperture radar imaging," *IEEE Transactions on Quantum Engineering*, vol. 3, pp. 1–20, 2022.
[5] A. King and W. Bernoudy, "Performance benefits of increased qubit connectivity in quantum annealing 3-dimensional spin glasses." doi: 10.48550/ARXIV.2009.12479., 2020.
[6] K. Perlin, "An image synthesizer," *ACM Siggraph Computer Graphics*, vol. 19, no. 3, pp. 287–296, 1985.

TABLE I
Embedding Properties

Embedding Type	**Chain Length** *Avg*	*STD*	*Max*	**Average *Accuracy***
This work	1	0	1	99
Auto 1	1.890	1.024	5	64.4
Auto 2	1.595	0.782	4	78.4
Auto 3	1.830	0.825	4	57
Auto 4	1.685	0.804	4	57
Auto 5	1.795	0.783	4	41.4